

See discussions, stats, and author profiles for this publication at: <https://www.researchgate.net/publication/273519699>

Effects of Particle Size and Shape on the Performance of a Trickle Fixed-Bed Recycle Reactor for Fischer-Tropsch Synthesis

ARTICLE in INDUSTRIAL & ENGINEERING CHEMISTRY RESEARCH · FEBRUARY 2015

Impact Factor: 2.59 · DOI: 10.1021/ie503174v

CITATION

1

READS

42

7 AUTHORS, INCLUDING:



Kyle M. Brunner

5 PUBLICATIONS 8 CITATIONS

SEE PROFILE



Robson Peguin

Braskem

21 PUBLICATIONS 154 CITATIONS

SEE PROFILE



Calvin Bartholomew

Brigham Young University - Provo Main Campus

188 PUBLICATIONS 7,285 CITATIONS

SEE PROFILE



William C. Hecker

Brigham Young University - Provo Main Campus

103 PUBLICATIONS 1,007 CITATIONS

SEE PROFILE

Effects of Particle Size and Shape on the Performance of a Trickle Fixed-Bed Recycle Reactor for Fischer–Tropsch Synthesis

Kyle M. Brunner, Hector D. Perez, Robson P. S. Peguin, Joshua C. Duncan, Luke D. Harrison, Calvin H. Bartholomew, and William C. Hecker*

Department of Chemical Engineering, Brigham Young University, Provo, Utah 84602, United States

ABSTRACT: A previously developed one-dimensional reactor model was employed to understand the effects of pellet size and geometry on the performance of a wall-cooled multitubular fixed-bed Fischer–Tropsch reactor for producing hydrocarbons from synthesis gas. The effects of pellet size/shape on catalyst effectiveness, bed void fraction, and overall heat transfer coefficient were studied through a comprehensive parametric study of a reactor with cobalt catalyst. The relative impact of each of these parameters on the overall required amount of catalyst was also determined. The simulations show that the amount of catalyst required to achieve a specified conversion increases with pellet size and shape in the order: trilobes < hollow cylinders < cylinders < spheres. The pressure drop per unit length can be significantly reduced and the catalyst effectiveness increased by using advanced extrudates, i.e., trilobes or hollow cylinders.

1. INTRODUCTION

Reactor design, construction, and operation are among the most significant costs in building and running a Fischer–Tropsch Synthesis (FTS) plant. Minimizing these costs has been increasingly aided through validated computer models developed in the past two decades. These models have been used to relate process and design conditions to reactor performance, and thus allow a more reliable approach to reactor scale up and optimization. Wang et al. developed a 1-D heterogeneous reactor model for iron catalysts that uses a highly detailed kinetic model (14 parameters),¹ a comprehensive pellet model,² and a modified SRK equation of state specific to FTS that predicts the individual species produced on an active Fe–Cu–K catalyst.³ Jess and Kern⁴ used a pseudohomogeneous 2-D model to simulate FTS performance of both cobalt and iron catalysts in nitrogen-rich syngas. The Wang et al. and Jess and Kern models describe the effects of process parameters such as tube diameter, recycle ratio, pressure, and cooling temperature on FTS reactor performance. Although these models are good within their designed scope, they fail to show the effects of particle size and shape on reactor development.

Parametric studies on packed bed catalytic reactors reported in the literature indicate that the effects of parameters such as catalyst pellet size and shape should be considered during FTS studies. Though this should merit consideration, a comprehensive study of these parameters has not yet been performed. Studies up until now have reported on the effects of particle shape and size on parameters such as pressure drop, liquid holdup, effectiveness factor, and required bed length. Bazmi et al.⁵ reported that pressure drop in trickle bed reactors with randomly packed spheres is greater than for randomly packed trilobes at a variety of gas and liquid fluxes, with this difference becoming more pronounced at greater fluxes. Cylinder extrudates were reported to result in packed bed pressure drops that are higher than those for hollow cylinders and lower than those for spheres.^{6,7} It is widely accepted that increases in

catalyst pellet size result in lower reactor pressure drops due to higher bed void fractions. Trividakis et al.⁸ also reported that larger pellet sizes result in smaller liquid holdups, which impact the mass and heat transfer resistances for FTS and explain why these pellet sizes result in lower pressure drops. In terms of kinetics, the effectiveness factor of steam reforming catalysts of equivalent mass was found to increase with pellet shape in the following order: spheres < cylinders < hollow cylinders.⁷ Due to the increase in the effectiveness factor, hollow cylinder packing requires shorter bed lengths than do cylinders and spheres.

These results reported in the literature underline the need and potential value of a comprehensive study of the effects of catalyst pellet size and shape on FTS reactor performance and design. A model that can perform such a comprehensive study exists and has been developed previously by our lab.⁹ This model is a one-dimensional model for both iron and cobalt catalysts that includes recycle, accounts for radial heat transfer, predicts the behavior of trickle flow fixed-bed reactors, and has been validated with industrial data. The present model is the only known FTS computer model reported in the literature that has the flexibility of allowing the user to select from a variety of catalyst pellet shapes (spheres, cylinders, hollow cylinders, and trilobes) and sizes, among other parameters, for reactor simulation. The program goes beyond simply showing the effects of pellet shape and size on hydrodynamic properties by including the effects of these on both the heat transfer and kinetics of trickle flow Fischer–Tropsch (FT) systems. The purpose of this paper is to explore the effects of these two catalyst design parameters, pellet size and geometry, on FTS performance. This work reports the results for cobalt catalysts, and although a similar study has been done in our lab for iron

Received: August 9, 2014

Revised: February 13, 2015

Accepted: February 17, 2015

Published: February 17, 2015

catalysts,¹⁰ those results will not be presented here. In general, the trends observed for iron catalysts are similar to those observed for cobalt catalysts.

2. MODEL AND BASE CASE

2.1. Model Description. The fixed-bed reactor (FBR) modeled in this work consists of a multitubular shell and tube heat exchanger with catalyst pellets packed in the tubes and downstream hot and cold traps for product separation (see Figure 1). Conceptually, the reactor effluent containing liquid

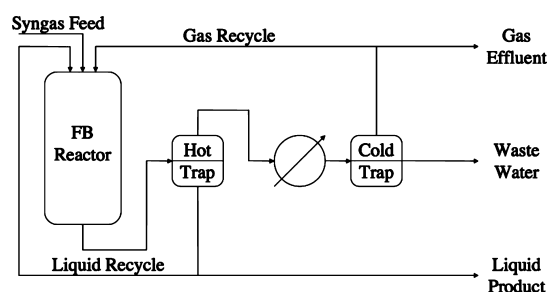


Figure 1. PFD of fixed-bed reactor with recycle for FTS.

wax products (C_{5+} hydrocarbons) and gaseous species (water, C_{2-4} hydrocarbons, and noncondensables) exits the reactor and flows into a hot trap where the wax products are separated from the gas. From the hot trap, the gas effluent enters a cold trap where the water, C_{2-4} , and oxygenated hydrocarbon species are separated from the noncondensable gases (H_2 , CO, CO_2 , and CH_4). Portions of the liquid wax and noncondensable gases are recycled to the reactor. The gas recycle ratio is defined as the molar flow ratio of the recycled stream to the gas effluent stream. It is assumed that all water is removed at the reactor exit and is not included in the gas recycle. The liquid recycle ratio is defined as the molar flow ratio of the liquid recycle to the liquid tail stream.

The reactor model was developed with a simplified, fixed selectivity model in which the user specifies the fractions of reacted carbon monoxide that are converted to methane, gaseous light hydrocarbons (C_{2-4}), liquid heavy hydrocarbons (C_{5+}), gaseous oxygenates, and carbon dioxide.⁹ The physicochemical properties of the hydrocarbon products are determined from the properties of propane for the C_{2-4} fraction and the properties of $C_{25}H_{52}$ for the C_{5+} fraction. Physicochemical properties of the oxygenated fraction are determined from the properties of methanol.

For each simulation, the reactor design equations for mass, energy, and momentum given by Davis and Davis¹¹ (eqs 1 and 2) and Froment and Bischoff¹² (eq 3) are solved numerically using a fourth-order Runge–Kutta method.¹³ The model solves these equations by stepping down the length of the reactor bed (default step size of 3.0 mm) until a user-specified CO conversion is reached (60% by default).

$$-\frac{dF_A}{dz} = A_{cs}\eta\rho_b(-r_{CO}) \quad (1)$$

$$\mu\rho_c\frac{dT}{dz} = (-\Delta H_{rxn|T})\eta\rho_b(-r_{CO}) - \frac{4U}{d_t}(T - T_{wall}) \quad (2)$$

$$\frac{dP}{dz} = \frac{\delta_{GW}}{\left(1 - \frac{\epsilon_{l,dyn}}{\epsilon_b}\right)^3} - \rho_g g \quad (3)$$

The reactor model uses the correlation developed by Benyahia and O'Neill¹⁴ (eq 4) to calculate the reactor bed void fraction, ϵ_b . The correlation depends on sphericity, defined as the ratio of the surface area of a sphere of equivalent volume to the surface area of the pellet.

$$\epsilon_b = 0.1504 + \frac{0.2024}{\phi_p} + \frac{1.0814}{(d_t/d_{pe} + 0.1226)^2} \quad (4)$$

For the pressure drop predictions (eqs 3 and 5), the Tallmadge¹⁵ equation (eq 7) is used to calculate friction factor and an equation attributed to Satterfield and reported elsewhere^{10,12} is used to calculate dynamic liquid holdup ($\epsilon_{l,dyn}$). Dynamic liquid holdup $\epsilon_{l,dyn} = (\mu_l u_l)/d_p^2 g \rho_l$

$$\delta_{GW} = \frac{1 - \epsilon_w}{\epsilon_w^3} \frac{\rho_g u_g^2}{d_{pe}} f \quad (5)$$

$$\epsilon_w = \epsilon_b - \epsilon_{l,stat} \quad (6)$$

In this study a value of 0.035 was used for the static liquid holdup.¹²

$$f = 4.2 \left(\frac{1 - \epsilon_b}{Re_g} \right)^{1/6} + \frac{150(1 - \epsilon_b)}{Re_g} \quad (7)$$

The reactor model was developed with the ability to accept a large variety of kinetic expressions, including Langmuir–Hinshelwood, Eley–Rideal, and power law models. Equation 8 shows the kinetic expression used in this study for the cobalt base case, with units of $\text{mol}_{CO}/\text{mol}_{site}/s$ (partial pressures in atm and temperature in K).⁹

$$-r_{CO} = \frac{142e^{-4.070/T} P_{CO}^{0.5} P_{H_2}^{0.5}}{(1 + 1 \times 10^{-9} e^{9.440/T} P_{CO} + 0.0024e^{2.150/T} P_{H_2}^{0.5})^2} \quad (8)$$

The effectiveness factor and Thiele modulus for the catalyst pellets are determined from the relationships in eqs 9 and 10. The effectiveness factor accounts for diffusion resistance within the pellet and is defined as the ratio of the observed to the intrinsic rates of reaction. An average effective reaction order, n_{ro} , is indicated in eq 10 and is typically determined as the average CO reaction order over the range of conditions studied. We used a value of -0.1 as the base case value for cobalt catalyst in this study.

$$\eta = \frac{\tanh(\phi)}{\phi} \quad (9)$$

$$\phi = L_p \sqrt{\frac{k_e C_A^{n_{ro}} (n_{ro} + 1)}{2D_e C_A}} \quad (10)$$

Heat transfer down the length of the reactor is modeled according to eqs 11 to 14^{12,16} as reported in the previous study.⁹

$$\frac{1}{U} = \frac{1}{h_{wall}} + \frac{d_t}{8\lambda_{er}} \quad (11)$$

$$\lambda_{er} = 1.5\lambda_1 + (\alpha\beta)_g G_g c_{p,g} d_{pe} + (\alpha\beta)_l G_l c_{p,l} d_{pe} \quad (12)$$

$$h_{wall} = \frac{10.21\lambda_{er}^s}{d_t^{4/3}} + 0.033 \frac{\lambda_g}{d_p} Pr_g Re_g \quad (13)$$

$$Re_g = \frac{G_g d_p}{\mu_g} \quad (14)$$

Note: All variables are defined at the end of the text.

2.2. Base Case. The present study of the response of reactor performance to varied catalyst size and geometry uses a standard set of conditions against which all other results are compared. The standard conditions for cobalt in this work are representative of the first stage of a biofuels-to-liquids plant, i.e., a plant with productivity of 500 bbl/day operating at a CO conversion (X_{CO}) of 60%. The standard conditions used for this study are given in Table 1 and the simulation results for these conditions are reported in Table 2.

Table 1. Base Case for Cobalt Catalysts^a

inputs	value
flow rate (SCFH) $\times 10^{-5}$	10.1
feed mol % of CO	28.5
feed mol % of H ₂	59.5
feed mol % of N ₂	12.0
inlet temperature (K)	484
wall temperature (K)	478
inlet pressure (atm)	40
gas recycle ratio ^b	2.0
liquid recycle ratio ^b	0.5
final CO conversion	0.60
selectivity to CH ₄	0.050
selectivity to C ₂₋₄	0.080
selectivity to C ₅₊	0.860
selectivity to oxygenates	0.010
selectivity to CO ₂	0.000
reaction order ^c	-0.1
catalyst activity	1
number of tubes	1,300
tube inner diameter (mm)	25.4
pellet diameter (mm)	1.3
pellet geometry	trilobe
pellet aspect ratio ^d	3.5
pellet pore volume (cm ³ g ⁻¹)	0.42
bulk density (kg m ⁻³)	600

^aConditions represent plants operating at 60% CO conversion with productivity of 500 bbl/day. ^bRecycle/tailgas ratio. ^cFor Thiele modulus calculation. ^dPellet length/ d_p .

2.3. Catalyst Shapes. The four catalyst shapes used in the reactor model and this study are depicted in Figure 2. The dimensions of the pellets can be varied by the user. An aspect ratio of 3.5 is used for the extrudates in this study, but can also be varied.

2.4. Effective Pellet Diameter. In order to perform a fair comparison of catalyst geometries, pellet diameter (d_p) studies are based on effective pellet diameter (d_{pe}). Effective pellet diameter is the diameter of a sphere having the same catalyst volume as the actual pellet. This allows for a normalized comparison since spheres cannot be directly compared to extrudates due to the disparity (roughly equal to the aspect

Table 2. Results Predicted under Base Case Conditions for Cobalt Catalysts

predicted values	value
outlet temperature (K)	492
max temperature (K)	493
HT coefficient (W m ⁻² K ⁻¹)	1114
cooling duty (MW)	9.8
reactor length (m)	6.1
mass of catalyst (kg)	2425
pellet density (kg m ⁻³)	1159
void fraction	0.48
pressure drop (atm)	3.86
productivity (g _{HC} g _{cat} ⁻¹ h ⁻¹)	1.08
avg. effectiveness factor	0.77

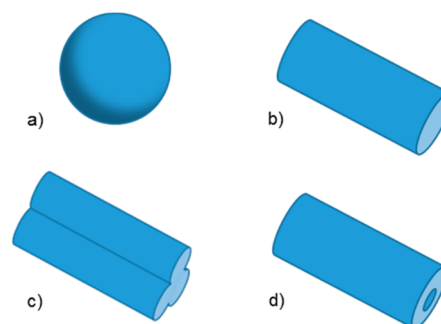


Figure 2. Four pellet shapes used in the reactor model: (a) spheres, (b) cylinders, (c) trilobes, and (d) hollow cylinders.

ratio) in pellet masses and surface areas of the same diameter. Table 3 gives actual pellet diameters for the shapes used in this

Table 3. Actual d_p Values of Pellet Shapes Used in This Study for Given Effective Spherical Pellet Diameters (d_{pe})

d_{pe} (mm)	d_p (mm) ^a			
sphere	cylinder	h. cyl. ^b	trilobe	
0.5	0.29	0.3	0.32	
1	0.58	0.6	0.65	
2	1.15	1.2	1.29	
4	2.3	2.39	2.58	
8	4.6	4.79	5.17	
16	9.21	9.58	10.3	

^aAspect ratio = 3.5. ^bInner diameter = $d_p/3$.

study along with their corresponding effective spherical pellet diameters. Pellet shape and effective diameter were then varied in the following studies to explore their effects on model predictions. The average temperature (T_{avg}) was also maintained at 492 K by varying the cooling temperature (T_{wall}). This allowed for these studies to focus on the effects of shape and size, rather than the effects of additional variables such as temperature.

3. MODEL PREDICTIONS AND DISCUSSION

The model described previously can be used to accurately predict FT reactor response to changes in catalyst pellet size and geometry. Reactor response around common operating conditions for cobalt catalysts is observed in a series of parametric runs for each variable. The effect of pellet size and shape on catalyst effectiveness, bed void fraction, and overall

heat transfer coefficient are presented and discussed in the following sections.

The ideal packed bed minimizes pressure drop (ΔP) and reduces the required bed length (L_{bed}) for a specified conversion, without compromising the catalyst mechanical strength. A significant challenge in accomplishing these objectives results from the trade-off between the effects of catalyst geometry on each of these ideals. For example, as pellet diameter decreases, bed void fraction also decreases, leading to greater pressure drop and resistance to fluid flow. On the other hand, small pellet diameters improve pore diffusion (decrease the pellet effective diffusion length, L_{pe}) and thus increase observed reaction rate. Using smaller pellets can be a problem because they are prone to being crushed and creating fines in packed beds due to their reduced mechanical strength. Crushed fines are undesirable as they hinder gas flow further and require a halt in operations to replace the catalyst. The objective then is to find pellet shapes and sizes that optimize diffusion resistance and ϵ_b to give the lowest ΔP and highest reaction rate (for shortest bed length and lowest catalyst weight, W_{cat}).

3.1. Physical Properties of Pellet Geometries. Table 4 summarizes the physical properties, including surface area,

Table 4. Properties for 2 mm Diameter Pellets of Four Pellet Geometries (Reactor Tube Inner Diameter = 25.4 mm, Aspect Ratio = 3.5)

shape	surface area (mm ²)	sphericity	bed void fraction	diffusion length (mm)
sphere	12.6	1	0.359	$d_p/6$
cylinder	50.3	0.755	0.438	$d_p/4$
h. cyl. ^a	64.2	0.546	0.539	$(d_p - d_i)/4$
trilobe	48.4	0.622	0.491	$d_p/8$

^aInner diameter $d_i = d_p/3$

sphericity, bed void fraction, and diffusion length of the four pellet shapes of this study (spheres (S), cylinders (C), hollow cylinders (hC), and trilobes (Tr)), each with diameters of 2 mm (extrudates have aspect ratios of 3.5). As shown in this table, trilobes have both a larger bed void fraction (0.49 compared with 0.44) and half the effective diffusion length (0.25 mm compared to 0.5 mm) of cylinders with the same diameter. This results in an overall decrease in pressure drop and increase in kinetics (rate). Advanced pellet geometries (e.g., trilobes) offer a compromise between effective diffusion length and pellet diameter, which is beneficial in obtaining the desired characteristics for the ideal packed bed discussed in the section above.

3.2. Overall Effect on Required Catalyst Mass and Reactor Length. The parametric studies performed show that increasing d_{pe} increases the catalyst mass, W_{cat} , required to maintain the same CO conversion and C_{S+} production rate (see Figure 3). For a given d_{pe} , the required W_{cat} decreases with catalyst shape in the order spheres > cylinders > hollow cylinders > trilobes. These results are in agreement with those presented by Soltan Mohammadzadeh and Zamaniyan for steam reforming catalysts.⁷ In their study, the authors report that for the same catalyst mass, spheres and cylinders have methane conversions of about 70%, whereas hollow cylinders have conversions of about 80%. The fact that the conversion for cylindrical pellets was not greater than for spheres can be accounted for by the slightly greater effective pellet diameter of the former (19.5 mm vs 17.0 mm). As expected, the required

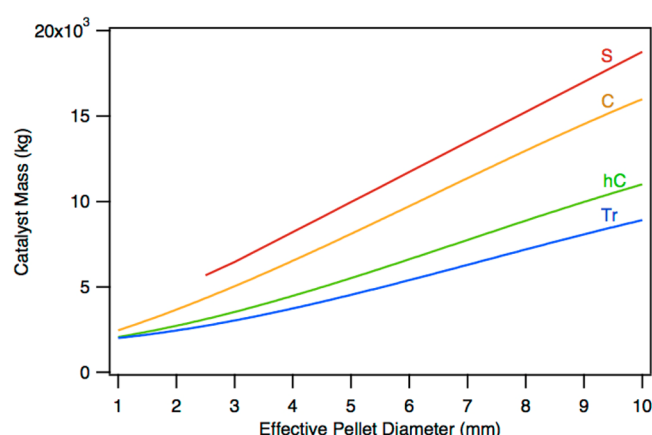


Figure 3. Effect of d_{pe} and pellet shape on W_{cat} required to achieve $X_{\text{CO}} = 0.60$ for the Co base case; T_{wall} varied to keep $T_{\text{avg}} = 492$ K.

catalyst weight tends to be similar for all shapes when the effective pellet diameter is decreased, thus minimizing shape differences.

Model simulations were also run to quantify the overall effect of pellet shape and size on the reactor bed length, using a fixed pellet density of 1159 kg/m³ (rather than a fixed bed density). For a given W_{cat} , the bed length depends on the bed density, ρ_b , which is related to ϵ_b and pellet density, ρ_p , by eq 15.

$$\rho_b = \rho_p (1 - \epsilon_b) \quad (15)$$

Figure 4 shows the increase in bed length with d_{pe} necessary to achieve the base case CO conversion (60%). This figure is

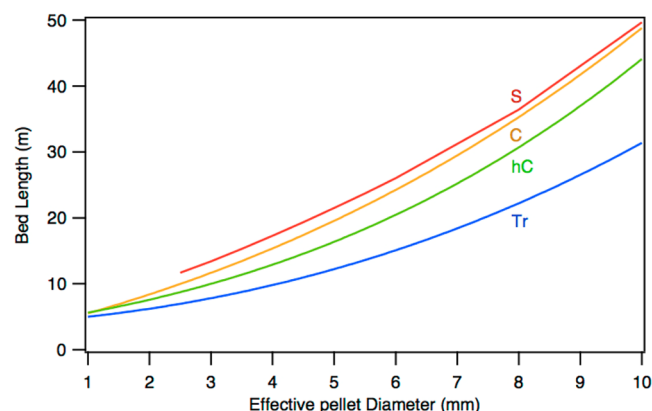


Figure 4. Effect of d_{pe} and shape on L_{bed} to achieve $X_{\text{CO}} = 0.60$ for the Co base case; T_{wall} varied to keep $T_{\text{avg}} = 492$ K.

similar to Figure 3, except that Figure 4 shows more curvature due to the influence of ϵ_b on ρ_b . Due to this void fraction effect, there is a greater difference between trilobes and hollow cylinders and a lesser difference between spheres and cylinders. This further supports the similarity between the CO conversions for spheres and cylinders, using constant pellet density, reported by Soltan Mohammadzadeh and Zamaniyan.⁷

Although Figures 3 and 4 show the overall effect of pellet size and geometry on reactor performance/design, it is important to understand the fundamental principles that account for these trends. The results plotted in these figures arise from a combination of the effects of several other variables that are affected by d_{pe} and shape. The following discussion considers the individual contributions of bed void fraction, pressure drop,

catalyst effectiveness, and heat transfer to the overall effect of pellet shape and size on W_{cat} .

3.3. Effects on Pressure Drop. This section analyzes the effects of catalyst shape and size on the pressure drop per unit bed length ($\Delta P/L_{\text{bed}}$), which impacts the catalyst weight required to achieve a specified CO conversion. The pressure drop per length is dependent upon two main parameters that are functions of pellet shape and size: bed void fraction and gas flow Reynolds number. Afandizadeh and Foumeny⁶ reported that pressure drop is very sensitive to bed void fraction, being inversely proportional to the cubed value of the void fraction. The effect of the pellet size and shape on bed void fraction is shown in Figure 5 below. Void fraction increases with d_{pe} and

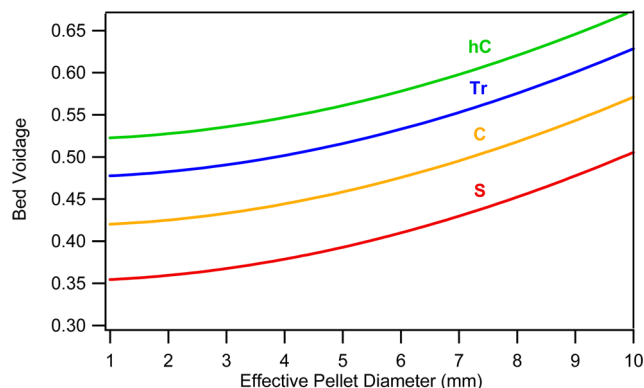


Figure 5. Effect of d_{pe} and shape on ε_b for the Co base case.

with shape in the order of spheres < cylinders < trilobes < hollow cylinders. The increase in ε_b is due in part to pellet–wall interactions which become significant for tube-to-effective-pellet-diameter ratios less than 20.¹⁷ The results shown in Figure 5 are consistent with Bazmi et al.,⁵ who report that trilobes of similar equivalent diameter (~ 1 mm) result in a greater bed void fraction relative to spheres (0.46 vs 0.41) in trickle beds with loose bulk density packing, which is the packing assumed by the present model. Soltan Mohammadzadeh and Zamaniyan⁷ also found similar results of increasing bed void fraction with particle shape for steam reforming catalysts: spheres < cylinders < hollow cylinders. The different possible orientations for trilobes and cylinders and the particle interpenetration in hollow cylinders are probably the main cause of larger bed voidage fractions observed for these pellet shapes relative to spheres. Afandizadeh and Foumeny reported conflicting results that show lower bed void fractions for cylinders relative to spheres (0.30 vs 0.40).⁶ This difference can be addressed by the packing structure assumed: Afandizadeh and Foumeny's work assumes dense packing, whereas the model used in this study assumes loose/random bed packing.

As shown by Figure 6, pellet diameter has a significant effect on the pressure drop in a reactor. For a given d_{pe} , the value of $\Delta P/L_{\text{bed}}$ with respect to shape decreases in the order spheres > cylinders > trilobes > hollow cylinders. $\Delta P/L_{\text{bed}}$ is seen to approach a minimum for all pellet shapes at large d_{pe} due to wall–pellet interactions and large void spaces. As a result, pellet shape only has a significant impact on pressure drop when $d_{\text{pe}} < 4$ mm, which is the pellet size range typical of FTS. Trivizadakis et al.⁸ reported that for $d_{\text{pe}} < 2$ mm, $\Delta P/L_{\text{bed}}$ increases significantly with decreasing d_{pe} . For example, pressure drop per unit length in reactors packed with spheres increases by 3-fold when pellet diameter is decreased from 2 to 1 mm (see Figure

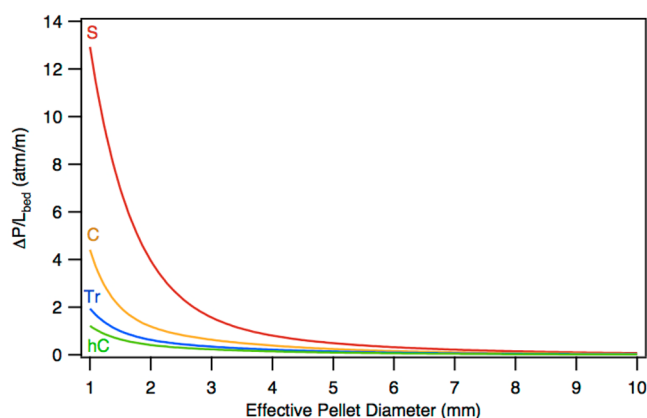


Figure 6. Effect of d_{pe} and shape on $\Delta P/L_{\text{bed}}$ for the Co base case; T_{wall} varied to keep $T_{\text{avg}} = 492$ K.

6). Figure 6 also shows that reactors packed with trilobes or hollow cylinders are less sensitive to changes in pellet diameter than those packed with spheres and cylinders. It is interesting to note that hollow cylinders result in the smallest pressure drop even though trilobes give lower W_{cat} and L_{pe} . This indicates that other factors beyond bed void fraction determine the overall impact of d_{pe} on W_{cat} .

3.4. Effects on Pore Diffusion. Pellet size and shape affect the observed reaction rate via the effectiveness factor, which depends on the pore diffusion length (see eqs 9 and 10). Figure 7 shows the effects of d_{pe} and shape on η : effectiveness factor

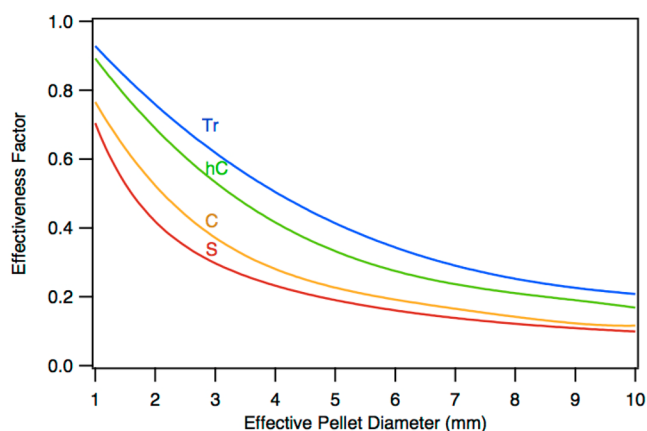


Figure 7. Effect of d_{pe} and shape on η for the Co base case; $T_{\text{avg}} = 492$ K (vary T_{wall}).

increases as d_{pe} decreases. This increase is more significant for $d_{\text{pe}} < 4$ mm, which is the size range of interest for FTS. At a certain d_{pe} , the order of increasing η with shape is spheres < cylinders < hollow cylinders < trilobes. The drop in effectiveness factor with increasing d_{pe} can be explained from an effective diffusion length standpoint. L_{pe} is the ratio of pellet volume to surface area and is an indication of the relative resistance to diffusion. As L_{pe} increases (increasing d_{pe}), diffusion resistance increases, η decreases, and the observed reaction rate decreases. A lower observed rate of reaction for larger d_{pe} results in a larger required catalyst weight and longer bed length.

3.5. Effects on Heat Transfer. It was found that the overall heat transfer coefficient (U) increases with increasing d_{pe} (see Figure 8). Previous studies show that the main heat transfer

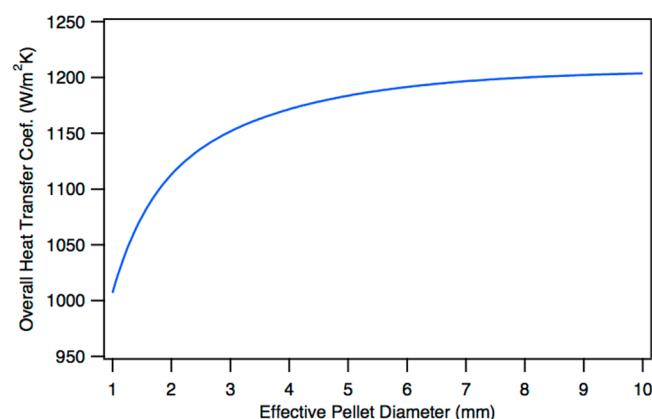


Figure 8. Effect of pellet diameter and shape on U with $T_{\text{avg}} = 492$ K (vary T_{wall}) for the Co base case.

resistance in a packed bed is at the wall.^{9,18,19} Heat transfer coefficients in trickle flow FBRs (two fluid phases) approach values of single phase correlations due to inherently low liquid flow rates and little liquid–wall interactions, indicating that gas–wall interactions and gas–bed mixing in the reactor are the most important heat transfer considerations. Thus, increasing d_{pe} increases U due to the increase in ϵ_b . The presence of larger voids promotes gaseous mixing at the wall and in the bed, thus favoring the heat transfer by convection. Increasing U contributes to more stable operation (better temperature control) and longer bed lengths necessary to achieve a specific CO conversion. Lower bed temperatures are achieved when the heat transfer resistance is reduced, which results in slower kinetics and longer required bed lengths. Thus, there is a trade-off between economics and catalyst performance/selectivity, which should be considered carefully by the designer. In general, optimal pellet sizes are those that decrease the required catalyst weight as much as possible (small d_{pe}), while maintaining proper temperature control.

3.6. Effects of Intermediate Parameters on W_{cat} . The previous sections have shown the effects of pellet shape and size on the three main parameters that affect W_{cat} (pressure drop, diffusion length, and heat transfer). This section analyzes the effects of these three parameters on W_{cat} to gain an understanding of the relative impact of each of these parameters. Five series of simulations were performed on trilobe catalysts by varying the effective pellet diameter to study these effects. These five scenarios are divided into two cases: (1) one at constant average temperature and (2) another at constant cooling water temperature. Case 1 is done to compare the effects all three parameters with the isolated effects of L_{pe} and $\Delta P/L_{\text{bed}}$. Case 2 is done to compare the cumulative effect of all three parameters with the isolated effect of U . For case 2, the average temperature is not held uniform for the different pellet sizes in order to capture the full effect of U on W_{cat} , as it is dependent on temperature. Table 5 summarizes the conditions for simulations in cases 1 and 2. The word “varies” denotes that the parameter was allowed to vary as the pellet diameter was changed. The notation “const.” denotes that the parameter was fixed at its value at $d_{\text{pe}} = 2$ mm for all simulations. This is done to exclude its contribution to W_{cat} .

The results of these tests are shown in Figures 9 and 10. These figures show that the isolated effect of L_{pe} is the most significant, as its effect of W_{cat} is the closest to the overall effect of all three parameters (cumulative effect). The results also

Table 5. Test Matrix for Determining the Effect of Intermediates on W_{cat} ^a

temperature	U	$\Delta P/L_{\text{bed}}$	L_{pe}	effect of
case 1: $T_{\text{avg}} = 492$ K	varies	varies	varies	all
	const.	const.	varies	L_{pe}
	varies	varies	const.	$\Delta P/L_{\text{bed}}$
case 2: $T_{\text{wall}} = 478$ K	varies	varies	varies	all
	varies	varies	const.	U

^a“Varies” denotes that the parameter is unconstrained; “const.” denotes that the parameter is constrained to its value at $d_{\text{pe}} = 2$ mm.

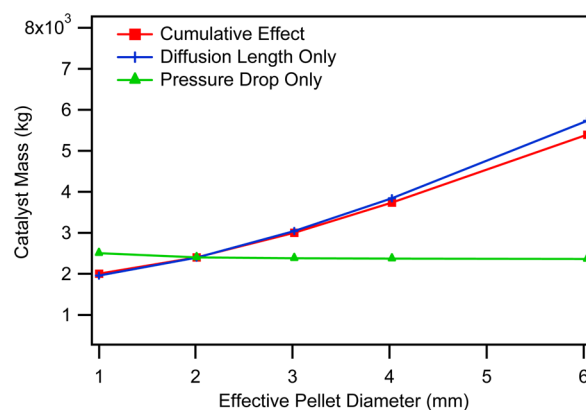


Figure 9. Comparison of the effect of $\Delta P/L_{\text{bed}}$ and L_{pe} on W_{cat} for case 1 (constant T_{avg}).

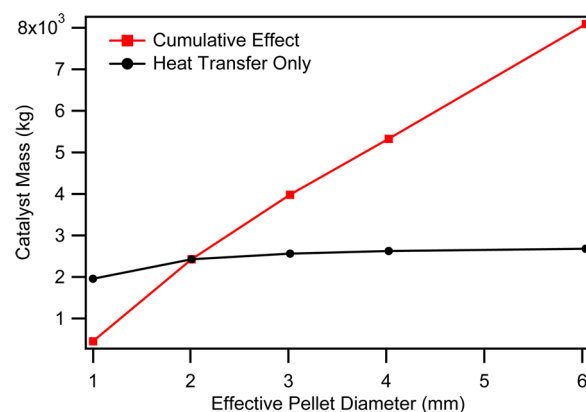


Figure 10. Effect of U on required W_{cat} for case 2 (constant T_{wall}).

show that the pressure drop effect is in the opposite direction as the effect of L_{pe} and U . For changes in effective pellet diameter in case 1 from 2 to 4 mm, the required catalyst mass increases by 56% for the cumulative effect and 61% for the isolated L_{pe} effect, but decreases for the isolated pressure drop effect by 1%. Figure 9 confirms the concept discussed earlier that larger pellet diameters lead to greater diffusion limitations but minimize pressure drop. Although there is a trade-off between the two, the dominating factor is the L_{pe} . For case 2, the increase for the cumulative effect on W_{cat} from 2 to 4 mm trilobes is of 120%, whereas the isolated heat transfer effect is only 8%. Thus, both the heat transfer and pressure drop effects are minor when compared to the effective diffusion length effect. This is a result of the direct effect of pellet thickness on the pore diffusion and thus on the observed reaction rate.

3.7. Schematic for the Effects of Pellet Size on the Required Catalyst Weight. An attempt to schematically

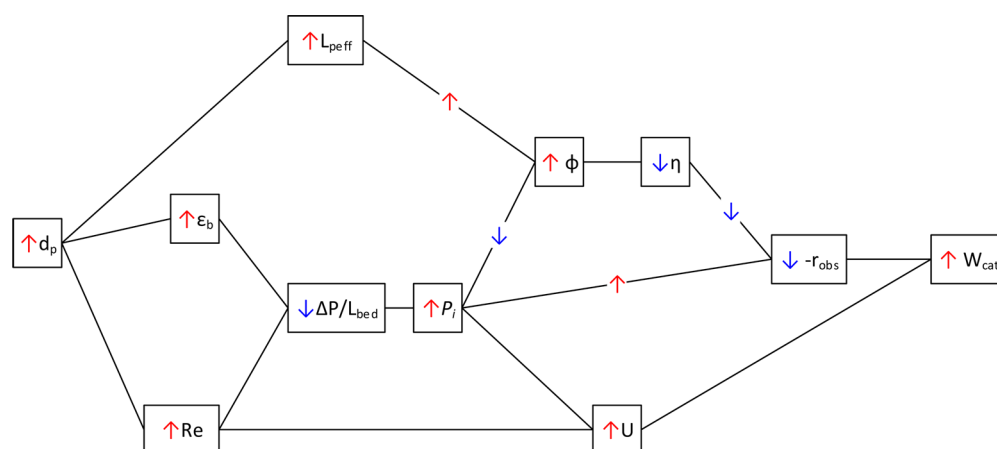


Figure 11. Schematic representation of the effect of pellet size on the different parameters that contribute to W_{cat} ; the direction of flow is from left to right.

represent the results from the previous sections for the effect of d_{pe} on the intermediate parameters, and then on to its overall effect on W_{cat} is given below in Figure 11. This schematic qualitatively shows the interactions between the different parameters that are affected by changes in pellet size, as well as their contributions to W_{cat} . The red arrows indicate that a certain parameter increases as a result of the change in the previous parameter. Blue arrows indicate a decrease in a certain parameter. For example, as d_{p} is increased, L_{pe} increases. Arrows on the connectors between different parameters indicate that there are competing effects with respect to other parameters. For example, an increase in L_{pe} tends to increase the Thiele modulus (ϕ), whereas an increase in axial partial pressures (P_i) has the opposite effect on ϕ . Overall, the effect of L_{pe} dominates the effect of the partial pressures and there is a net increase in ϕ .

4. CONCLUSIONS

A one-dimensional pseudohomogeneous multitubular trickle fixed-bed recycle reactor model for the Fischer–Tropsch synthesis was used in a series of parametric studies to better understand the effects of cobalt catalyst pellet size and shape on reactor design and performance. This study supports the following conclusions:

- The catalyst mass required to achieve a given conversion in a fixed bed FT reactor is linearly dependent on effective pellet diameter.
- Doubling the pellet size for effective diameters of 2.5 mm or more increases the required catalyst mass by at least 60%, with this increase being the largest for cylindrical pellets and smallest for trilobes.
- The required catalyst mass compared to spheres is 20% less for cylinders, 45% less for hollow cylinders, and 50% less for trilobes with effective diameters of 2.5 mm or more.
- Although trilobes minimize the catalyst weight and diffusion length, hollow cylinders minimize overall pressure drop.
- The pressure drop per unit length decreases with shape in the order: spheres > cylinders > trilobes > hollow cylinders (aspect ratio = 3.5). The pressure drop is most sensitive to pellet size for spheres and cylinders. As pellet diameter is decreased, the normalized pressure drop increases significantly for spheres (over 3-fold from 2 mm to 1 mm catalysts). This is also the case for cylinders, though to a lesser extent.

- The effectiveness factor decreases in the order: trilobes > hollow cylinders > cylinders > spheres.

- There is a trade-off between the effects of bed density and pressure drop on the required reactor bed length. For a decrease in pellet diameter, there is a decrease in bed void fraction, which increases the bed density and the pressure drop. Although, higher pressure drop contributes to greater required bed lengths, higher bed densities have the opposite effect. Decreasing pellet diameter also results in a smaller diffusion length, which overcomes the effect of pressure drop by the increase in the observed effectiveness factor.

- The rate of change of bed length with respect to effective pellet diameter is the lowest for trilobes.

- The bed void fraction decreases with catalyst shape in the order: hollow cylinders > trilobes > cylinders > spheres.

- Increasing pellet diameter increases the overall heat transfer coefficient by enhancing gas mixing within the bed and especially at the wall.

The effect of pellet size on the required amount of catalyst is the greatest through its effect on pore diffusivity, rather than on heat transfer or pressure drop.

Overall, this study shows the benefits in performing parametric studies on reactor design using the formulated model. These studies reveal that using advanced pellet geometries, mainly, trilobes, is advantageous because they optimize the trade-off between diffusion length and pressure drop. This facilitates minimizing the required catalyst mass to achieve a specified CO conversion. It is recommended that trilobes be used at the smallest size possible, which is greatly determined by their mechanical integrity under FTS conditions. The current state of the art size for these pellets is 1.3 mm diameters.²⁰ Also, trilobes maximize catalyst effectiveness by minimizing diffusion resistance, which is the single most important factor in reducing required catalyst mass. Consideration must be taken in ensuring that proper heat transfer is achieved, as smaller pellets result in a lower overall heat transfer coefficient.

■ AUTHOR INFORMATION

Corresponding Author

*E-mail: hecker@byu.edu.

Notes

The authors declare no competing financial interest.

■ ACKNOWLEDGMENTS

Financial support for this work has been provided by the members of the BYU Fischer–Tropsch Consortium. The authors would also like to thank Matt Svedin and Doug Tree who worked on early versions of the reactor code.

■ NOTATION

A_{cs} = cross sectional area of a tube
 c_p = specific heat capacity
 C_A = concentration of species A
 d_i = inner diameter (hollow cylinder)
 d_p = diameter of the pellet
 d_t = inner diameter of the tube
 D = diffusivity
 f = friction factor
 F_A = molar flow rate of species A
 F_A^0 = initial molar flow rate of species A
 g = gravitational constant
 G = superficial mass velocity
 h_{wall} = effective heat transfer coefficient at the wall
 L_{bed} = reactor bed length
 L_{pe} = effective diffusion length
 n_{ro} = effective reaction order for Thiele modulus calculation
 ΔP = pressure drop of gas in the reactor
 P = pressure
 P_i = partial pressure of species i
 Pr = Prandtl number
 $-r_{CO}$ = intrinsic rate of consumption of CO
 Re = Reynolds number
 T = temperature
 T_{avg} = average temperature
 T_{wall} = temperature of the tube wall
 u = superficial fluid velocity
 U = overall heat transfer coefficient
 \bar{V} = specific volume
 W_{cat} = catalyst weight
 X_A = conversion of species A
 z = reactor length

Greek Letters

$(\alpha \beta)$ = dynamic thermal conductivity coefficient
 $\Delta H_{rxn/T^0}$ = heat of reaction at reactor feed temperature
 δ_{GW} = pressure drop for gas flowing through a packed bed
 ϵ_b = void fraction of the bed
 $\epsilon_{l,dyn}$ = dynamic liquid holdup
 $\epsilon_{l,stat}$ = static liquid holdup
 ϵ_w = void fraction adjusted for the static liquid holdup
 φ = Thiele modulus
 φ_p = pellet sphericity
 η = overall effectiveness factor
 λ = thermal conductivity
 λ_{er} = effective radial thermal conductivity
 λ_{er}^s = static contribution to thermal conductivity
 μ = viscosity
 ρ = density
 ρ_b = bed density
 ρ_p = pellet density

Subscripts

e = indicates an effective property (effective diameter, effective diffusivity, etc.)
g = property of the gas
l = property of the liquid
s = property of the solid

■ REFERENCES

- (1) Wang, Y.; Xu, Y.; Li, Y.; Zhao, Y.; Zhang, B. Heterogeneous Modeling for Fixed-Bed Fischer–Tropsch Synthesis: Reactor Model and Its Applications. *Chem. Eng. Sci.* **2003**, *58*, 867–875.
- (2) Wang, Y.; Xu, Y.; Xiang, H.; Li, Y.; Zhang, B. Modeling of Catalyst Pellets for Fischer–Tropsch Synthesis. *Ind. Eng. Chem. Res.* **2001**, *40*, 4324–4335.
- (3) Wang, Y.; Li, Y.; Zhao, Y.; Zhang, B. Study On Solubility Correlation of Gases and Liquid Waxes Systems In Fischer–Tropsch Synthesis. *Tianranqui Huagong* **1999**, *24*, 48–53.
- (4) Jess, A.; Kern, C. Modeling of Multi-Tubular Reactors for Fischer–Tropsch Synthesis. *Chem. Eng. Technol.* **2009**, *32*, 1164–1175.
- (5) Bazmi, M.; Hashemabadi, S. H.; Bayat, M. Extrudate Trilobe Catalyst and Loading Effects on Pressure Drop and Dynamic Liquid Holdup in Porous Media of Trickle Bed Reactors. *Transp. Porous Media* **2013**, *99*, 535–553.
- (6) Afandizadeh, S.; Foumeny, E. A. Design of packed bed reactors: guides to catalyst shape, size, and loading selection. *Appl. Thermal Eng.* **2001**, *21*, 669–682.
- (7) Soltan Mohammadzadeh, J. S.; Zamaniyan, A. Catalyst Shape As A Design Parameter—Optimum Shape for Methane–Steam Reforming Catalyst. *Chem. Eng. Res. Des.* **2002**, *80* (4), 383–391.
- (8) Trivizidakis, M. E.; Giakoumakis, D.; Karabelas, A. J. A study of particle shape and size effects on hydrodynamic parameters of trickle beds. *Chem. Eng. Sci.* **2006**, *61*, 5534–5543.
- (9) Brunner, K. M.; Duncan, J. C.; Harrison, L. D.; Pratt, K. E.; Peguin, R. P. S.; Bartholomew, C. H.; Hecker, W. C. A Trickle Fixed-Bed Recycle Reactor Model for the Fischer–Tropsch Synthesis. *Int. J. Chem. React. Eng.* **2012**, *10* (1), 1–36.
- (10) Brunner, K. M. Novel Iron Catalyst and Fixed-Bed Reactor Model for the Fischer–Tropsch Synthesis. Ph.D. Dissertation, Brigham Young University: Provo, UT, 2012.
- (11) Davis, M. E.; Davis, R. J. *Fundamentals of Chemical Reaction Engineering*; McGraw Hill: Boston, 2003.
- (12) Froment, G. F.; Bischoff, K. B. *Chemical Reactor Analysis and Design*; John Wiley & Sons: New York, 1990.
- (13) Chapra, S. C.; Canale, R. P. *Numerical Methods for Engineers*; McGraw Hill: Boston, 2006.
- (14) Benyahia, F.; O'Neill, K. E. Enhanced voidage correlations for packed beds of various particle shapes and sizes. *Part. Sci. Technol.* **2005**, *23*, 169–177.
- (15) Tallmadge, J. A. Packed bed pressure drop—an extension to higher reynolds numbers. *AIChE J.* **1970**, *16*, 1092–1093.
- (16) Matsuura, A.; Hitaka, Y.; Akehata, T.; Shirai, T. Effective radial thermal conductivity in packed beds with gas-liquid downflow. *Heat Transfer – Jpn. Res.* **1979**, *8*, 44–52.
- (17) Harrison, L. D.; Brunner, K. M.; Hecker, W. C. A Combined Packed-Bed Friction Factor Equation: Extension to Higher Reynolds Number with Wall Effects. *AIChE J.* **2013**, *59* (3), 703–706.
- (18) Habtu, N.; Font, J.; Fortuny, A.; Bengoa, C.; Fabregat, A.; Haure, P.; Ayude, A.; Stüber, F. Heat transfer in trickle bed column with constant and modulated feed temperature: Experiments and modeling. *Chem. Eng. Sci.* **2011**, *66* (14), 3358–3368.
- (19) Specchia, V.; Baldi, G. Heat Transfer in Trickle-Bed Reactors. *Chem. Eng. Commun.* **1979**, *3*, 483–499.
- (20) LeViness, S. Velocys, Houston, TX. Personal communication, 2013.